Hypoxia Remediation and Methane Emission Manipulation Using Surface Oxygen Nanobubbles

Wenqing Shi[†,§], Gang Pan[*,†,‡], Qiuwen Chen[*,§], Lirong Song[//], Lin Zhu[⊥], Xiaonan Ji[†]

[†]Research Center for Eco-Environmental Sciences, Chinese Academy of Sciences, Beijing 100085, China

[‡]School of Animal, Rural, and Environmental Sciences, Nottingham Trent University, NG25 0QF, UK

[§]Center for Eco-Environment Research, Nanjing Hydraulic Research Institute, Nanjing 210098, China

[//]Institute of Hydrobiology, Chinese Academy of Sciences, Wuhan 430075, China

[⊥]School of Environmental Science & Engineering, Nanjing University of Information Science & Technology, Nanjing 210044, China

[*]Corresponding author: Tel: +86-10-62849686; Fax: +86-10-62923541; Email: gpan@rcees.ac.cn, or qwchen@nhri.cn

Abstract: Algal blooms in eutrophic waters often induce anoxia/hypoxia and enhance methane (CH_4) emissions to the atmosphere, which may contribute to global warming. At present, there are very few strategies available to combat this problem. In this study, surface oxygen nanobubbles were tested as a novel approach for anoxia/hypoxia remediation and CH_4 emission control. Incubation column experiments were conducted using sediment and water samples taken from Lake Taihu, China. The results indicated that algae-induced anoxia/hypoxia could be reduced or reversed after oxygen nanobubbles were loaded onto zeolite microporous and delivered to anoxic sediment. Cumulated CH_4 emissions were also reduced by a factor of 3.2 compared to the control. This was mainly attributed to the manipulation of microbial processes using the surface oxygen nanobubbles, which potentially served as oxygen suppliers. The created oxygen enriched environment simultaneously decreased methanogen but increased methanotroph abundances, making a greater fraction of organic carbon recycled as carbon dioxide (CO_2) instead of CH_4. The CH_4/CO_2 emission ratio decreased to 3.4×10^{-3} in the presence of oxygen nanobubbles, compared with 11×10^{-3} in the control, and therefore the global warming potential was reduced. This study proposes a possible strategy for anoxia/hypoxia remediation and CH_4 emission control in algal bloom waters, which may benefit global warming mitigation.

34 **Table of Contents**

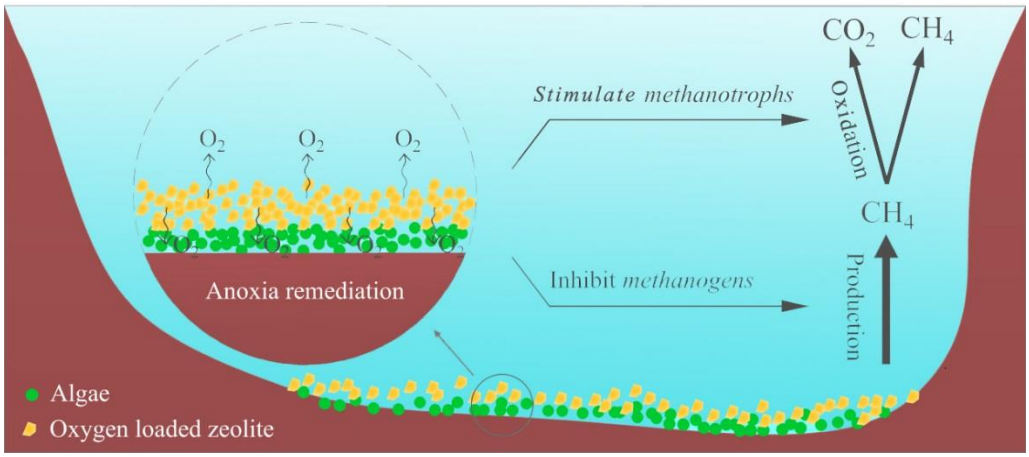

35
36

INTRODUCTION

In eutrophic waters, algae-induced anoxia/hypoxia is a serious environmental issue that can promote significant methane (CH_4) emission to the atmosphere.[1-3] Various strategies for adding oxygen directly into water to combat anoxia/hypoxia have been proposed.[4-7] However, the challenge is finding a safe and cost-effective method to deliver oxygen to anoxic/hypoxic areas, especially in deep waters. Downward pumping of oxygen-rich midwater was suggested as a solution to alleviate severe hypoxia that occurs annually in the Baltic Sea across an average area of 60×10^3 km^2.[8,9] Such an action would consume large amounts of energy and pose ecological risks resulting from disturbance to natural water turnover and circulation patterns.[8] There is therefore a need for an ecologically safe and cost-effective oxygen delivery technology that can remediate anoxia/hypoxia.

Nanobubbles are miniature gas bubbles with the diameters of < 200 nm that exhibit unique characteristics compared to macrobubbles.[10] The high stability and efficient gas solubility of oxygen nanobubbles make them potentially potent oxygen suppliers in water.[11] There are two types of nanobubbles, known as bulk and surface nanobubbles. Bulk nanobubbles are nanoscopic spherical bubbles dispersed in bulk liquids.[12] However, it still remains a challenge to deliver bulk oxygen nanobubbles to anoxic/hypoxic zones in deep waters as it consumes similar amount of energy as mixing through the use of pumps. Surface nanobubbles are nanoscopic gaseous domains at the solid-liquid interface.[13,14] Clay particles can act as potential carriers to deliver oxygen nanobubbles to targeted areas,[15,16] especially deep sediment via natural settling or hydraulic forces, which offers the prospect

of anoxia/hypoxia remediation in natural waters. This improvement of the aquatic environment may, in turn, affect microbial processes and achieve CH_4 emission control. However, such a principle has not yet been quantitatively tested.

In this study, we used an algal water-sediment simulation system to examine the use of surface oxygen nanobubbles in remediating algal anoxia/hypoxia and reducing CH_4 emission. Oxygen nanobubbles were loaded onto natural zeolite microsurfaces and delivered to bottom water after algae deposition. Zeolites without oxygen nanobubbles were used to identify the capping barrier effect of zeolites on gas emission. Dissolved oxygen (DO) in the water column, oxidation-reduction potential (ORP) at the sediment-water interface, and CH_4 as well as carbon dioxide (CO_2) fluxes across the water-air interface were measured over an incubation period of 20 d. The quantitative polymerase chain reaction (qPCR) method was also employed to analyze the responses of methanogens and methanotrophs in the systems which are responsible for CH_4 production and consumption, respectively.

MATERIALS AND METHODS

Oxygen Nanobubble Loaded Zeolites. Granular natural zeolites (1 ~ 3 mm in diameter) were placed into a pressure-resistant, airtight container and evacuated for 2 h (-0.08 MPa) using a vacuum pump (GM-1.0A, Tianjin Jinteng Experiment Equipment Co. Ltd., China) to remove air from zeolite pores. Oxygen gas was then added to the container (0.12 MPa) and maintained for 4 h. The oxygen nanobubble loaded zeolites were prepared freshly before use. The loaded oxygen was 20.5 mg g^{-1} zeolites, which was measured using the

sodium sulfite adsorption method (See Text S1 in the supporting information). Similarly, zeolites without oxygen nanobubbles were prepared by replacing oxygen gas with nitrogen gas.

Incubation Experiments. Approximately 35 L of sediment and 190 L of water samples were collected from Lake Taihu (China) using an Ekman grab sampler and a stainless-steel bucket, respectively, and then transported immediately to the laboratory in the dark. Both sediment and water samples were homogenized and then filled into cylinders (8.4 cm in diameter and 150 cm in height) to establish uniform sediment-water cylinders. In this study, twenty seven water-sediment cylinders were established. Each cylinder contained 15 cm of sediment and 120 cm of water column (Figure S2 in the supporting information). These cylinders were allowed to stand for two weeks before treatments. Fresh algal biomass was also collected at the same location as the sediment and water samples, and then freeze-dried (Beijing Boyikang Biological Experiment Equipment Co. Ltd., China) in the laboratory. To simulate algal-derived organic deposition, 0.4 g of dry algal biomass was added to each cylinder (60 mg dry weight/L water) and then settled with modified soil flocculants according to Shi et al. (2016) and Pan et al. (2011).[17,18] After algal deposition, nine cylinders were treated with 2-cm thick layer (110 ml in volume, 87 g in weight) of oxygen nanobubbles loaded zeolites (O-Ze) by adding them to the bottom water; and nine cylinders were treated with 2-cm thick layer (110 ml in volume, 87 g in weight) of zeolites without oxygen nanobubbles (Ze) to identify the capping barrier effect of zeolites on CH_4 emission. The control was run in nine simulation systems without any treatment after algal

deposition. Incubation experiments were conducted indoors at room temperature (22 ± 2°C) over a period of 20 d in the dark.

On day 0 (before the prepared cylinder ran), day 1, 3, 5, 7, 10, 13, 16 and 20, the changes of redox conditions and fluxes of CH_4 and CO_2 in these cylinders were analyzed, and 50 ml water samples were collected from an outlet of the cylinder (5 cm above the sediment-water interface) for DOC analysis. The DO in the overlying water was measured at 5 cm above the sediment-water interface using a DO meter (JPB-607A, Shanghai INESA Scientific Instrument Co. Ltd., China); and the ORP at the sediment-water interface was measured using an ORP meter (Orion 3-star, Thermo Fisher Scientific, USA). The water DOC was analyzed using a TOC analyzer (Liqui TOC II, Elementar, Germany). On day 0, 7 and 20, three cylinders in each treatment were randomly deposed to collect water and sediment samples for microbial analysis. The results were presented as the mean values. Water removed during sampling was replaced with surface water collected from Taihu Lake.

CH_4 and CO_2 Flux Analysis. Daily fluxes of CH_4 and CO_2 across the water-air interface in the cylinders were analyzed using a static micro-chamber method described by Duchemin et al. (1999).[19] On the sampling date, the micro-chamber was placed onto the water surface in each cylinder. Gas samples (10 ml) were collected before and after 2 h using a 25-ml polypropylene syringe. The samples were injected into a pre-evacuated Exetainer® vial for storage until analysis could be completed by gas chromatograph (7890B, Agilent Technologies, USA). Gas fluxes were calculated based on the changes in gas concentration over 2 h, and then total gas emissions were estimated throughout the 20-

day incubation.

Since CH_4 has a 25 times higher global warming potential (GWP) than CO_2 on a mass basis over a hundred year horizon,[20] carbon emissions with different CH_4/CO_2 ratios often differ in global warming impacts. Thus, the CH_4/CO_2 ratio has been commonly used as an important index for the study of carbon emissions from inland waters.[21] In this study, the CH_4/CO_2 ratio in each treatment was calculated by dividing CH_4 mass emission by CO_2 mass emission. Moreover, the total GWP of each treatment was also estimated and expressed in CO_2 equivalent. The conversion of CH_4 to CO_2 equivalent was conducted by multiplying CH_4 mass emission by a factor of 25.[20]

DNA Extraction and qPCR. Approximately 0.4 g of sediment samples were collected for sediment microbial analysis, and 800 mL water was collected from an outlet of the cylinder (5 cm above the sediment-water interface), and filtered through a 0.2 μm pore-size filters (Track-Etched Membranes, Whatman® Nuclepore™) for water microbial analysis. The sediment samples and filters were stored at -80°C before analysis. DNA extraction was undertaken with Powersoil DNA Isolation Kits and Powerwater DNA Isolation Kits (MoBio Laboratories Inc., Carlsbad, CA) according to the manufacturers' instructions, respectively; the DNA subsequently served as templates for qPCR amplification. The methanogens and methanotrophs in the samples were quantified using the qPCR method described below.

The qPCR assay was performed using primers targeting methanogenic archaeal 16S rRNA (primer set, 1106F/1378R) and methanotrophic *pmoA* genes (primer set,

142 A189F/M661R).[22-24]. Gene copies were amplified and quantified in a Bio-Rad cycler
143 equipped with the iQ5 real-time fluorescence detection system and software (version 2.0;
144 Bio-Rad). All reactions were completed in a total volume of 20 μL containing 10 μL
145 SYBR® *Premix Ex Taq*^{TM} (TOYOBO, Japan), 0.5 μM of each primer, 0.8 μL bovine serum
146 albumin (BSA, 3 mg/mL, Sigma), double distilled H_2O and template DNA. The qPCR
147 program for archaeal 16S rRNA was as follows: 95°C for 60 s, followed by 40 cycles of
148 95°C for 25 s and 57°C for 30 s and 72°C for 60 s. The qPCR program for *pomA*
149 commenced with 95°C for 60 s, followed by 40 cycles of 95°C for 25 s, 53°C for 30 s and
150 72°C for 60 s. The standard curve was established by a serial dilution (10^{-2} ~ 10^{-8}) of known
151 concentration plasmid DNA with the target fragment. All PCRs were run in triplicate on
152 96-well plates (Bio-Rad) sealed with optical-quality sealing tape (Bio-Rad). Three negative
153 controls without DNA template were included for each PCR run.

154 **RESULTS AND DISCUSSION**

155 **Anoxia/hypoxia Remediation.** In the control system, water DO decreased from 4.5 to 1.4
156 mg L^{-1} within the initial 7 d, and then gradually increased to 2.8 mg L^{-1} on day 20 (Figure
157 1A). Surface sediment suffered from severe anoxia, and the ORP at the sediment-water
158 interface remained below -200 mV throughout the experiment (Figure 1B). This
159 hypoxia/anoxia frequently occurs in eutrophic waters, which is often driven by algal
160 blooms.[25-28] When zeolites without oxygen nanobubbles were added (2-cm thick) after
161 algal deposition in the Ze treatment, the DO in the water column maintained a level of 3.6
162 ~ 4.9 mg L^{-1} throughout the 20-day incubation; and the ORP at the sediment-water interface

was reversed to +139.5 mV on day 1, and then decreased to -70.5 mV on day 20. Unlike anaerobic sediment, the zeolites that are in constant contact with air and sunshine are aerobic by nature. Thus, the ORP of the top layer sediment was quickly increased to become positive during the first few days after the capping (Figure 1B).[29] The zeolite capping layer can prevent oxygen-consuming materials in sediments enter into the overlying water, resulting in a relatively higher level of water DO in the Ze treatment than in the control. The remediation effect of zeolite addition was enhanced after the oxygen nanobubbles were loaded onto zeolites. After oxygen nanobubbles enriched zeolites were added (2-cm thick) in the O-Ze treatment, the DO in the water column was increased to 7.9 mg L^{-1} on day 1 and remained above 5.7 mg L^{-1} throughout the remaining incubation period (Figure 1A); and the ORP at the sediment-water interface was reversed to +189.0 mV on day 1 and remained positive throughout the experiment (Figure 1B).

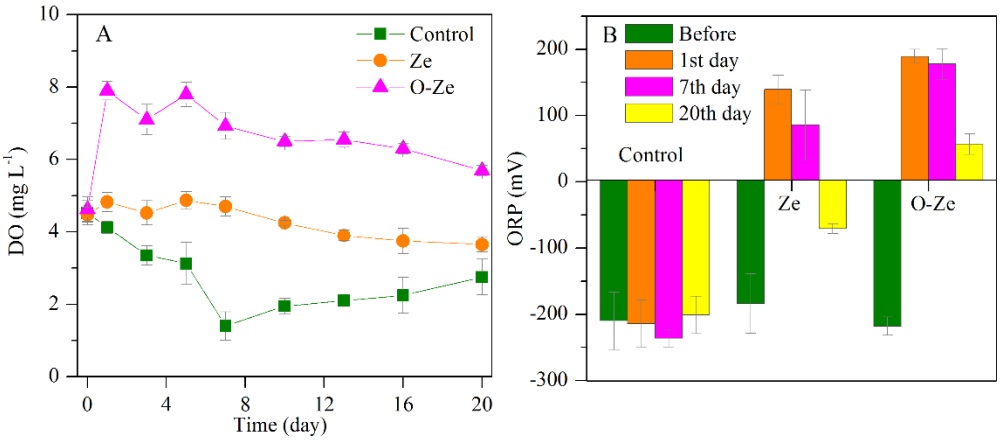

Figure 1. Water environment changes in the simulated column systems. (A) DO in water column. (B) ORP at the sediment-water interface. Control was run without any treatment after algal deposition; O-Ze and Ze represent the addition of zeolites with and without

oxygen nanobubbles after algal deposition, respectively. Error bars indicate standard deviations.

CH_4 Emission Mitigation. A significant CH_4 emission event occurred in the control system. The CH_4 flux across the water-air interface increased and reached a maximum of 215.3×10^{-3} g d^{-1} m^{-2} within the initial 7 d, with a cumulated CH_4 emission of 1.35 g m^{-2} over the 20 days period (Figure 2A). Although zeolite capping yielded a reasonably oxic water environment (Figure 1) in the Ze treatment, a cumulated CH_4 emission of 1.13 g m^{-2} was still detected over the 20-day incubation period. The CH_4 flux reached a maximum of 183.6×10^{-3} g d^{-1} m^{-2} on day 10. In contrast, when oxygen nanobubbles were loaded onto the zeolites and delivered to the bottom water in the O-Ze treatment, the cumulated CH_4 emission was reduced by a factor of 3.2 (0.32 g m^{-2}) compared to the control, and the maximum peak of CH_4 flux was 57.1×10^{-3} g d^{-1} m^{-2} on day 10 (Figure 2A). The CO_2 flux displayed a similar trend in each treatment, initially increasing due to algal organic carbon inputs, and then gradually decreasing to low steady levels as the organic carbon was consumed (Figure 2B); however, the CO_2 fluxes in the Ze and O-Ze were generally lower than in the control, which was potentially due to the capping barrier effect of zeolites carriers. It is important to note that, from day 4 to 16, the CO_2 flux in the O-Ze treatment was higher than that in the Ze treatment, whereas the CH_4 flux in O-Ze was lower than in the Ze (Figure 2A). Over the 20 days period, the cumulated CO_2 emissions were 119.3, 88.2 and 95.8 g m^{-2} in the control, Ze, and O-Ze treatments, respectively (Figure. 2B).

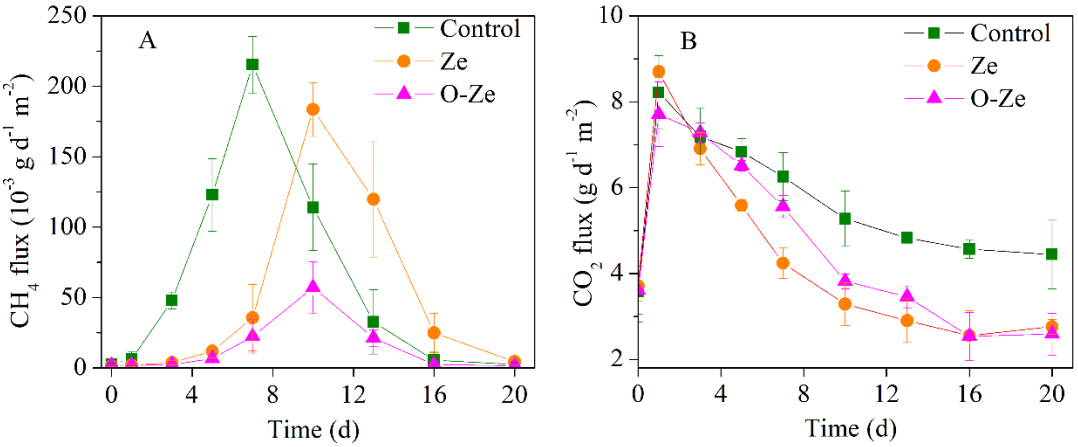

Figure 2. CH_4 and CO_2 fluxes across the water-air interface. (A) CH_4 fluxes. (B) CO_2 fluxes. The cumulated gas emissions over the 20-day incubation period were obtained by the trapezoidal method using MATLAB (MathWorks, USA).

In comparison with the control, the addition of zeolites without oxygen nanobubbles increased the CH_4/CO_2 emission ratio. Over the 20-day incubation period, the CH_4/CO_2 emission ratios reached 11×10^{-3} and 13×10^{-3} in the control and Ze treatments, respectively. In contrast, the use of oxygen nanobubbles enriched zeolites in the O-Ze treatment yielded a lower CH_4/CO_2 emission ratio of 3.4×10^{-3} (Figure 3A), suggesting that a greater fraction of organic carbon was recycled as CO_2 instead of CH_4 in the presence of the oxygen nanobubbles. This was in line with the fact that the CH_4 flux in the O-Ze treatment was lower than in the Ze treatment (Figure 2A), whereas the CO_2 flux was higher in the former than the latter (Figure 2B). As a result of the lower GWP of CO_2 relative to CH_4, the net global warming effect was reduced as a greater fraction of organic carbon was recycled as CO_2 instead of CH_4. Total GWP of the carbon emissions was 103.9 g m^{-2} (CO_2-eq) in the O-Ze treatment, as opposed to 153.1 g m^{-2} (CO_2-eq) in the control and 116.4 g

m^{-2} (CO_2-eq) in the Ze treatment (Figure 3B).

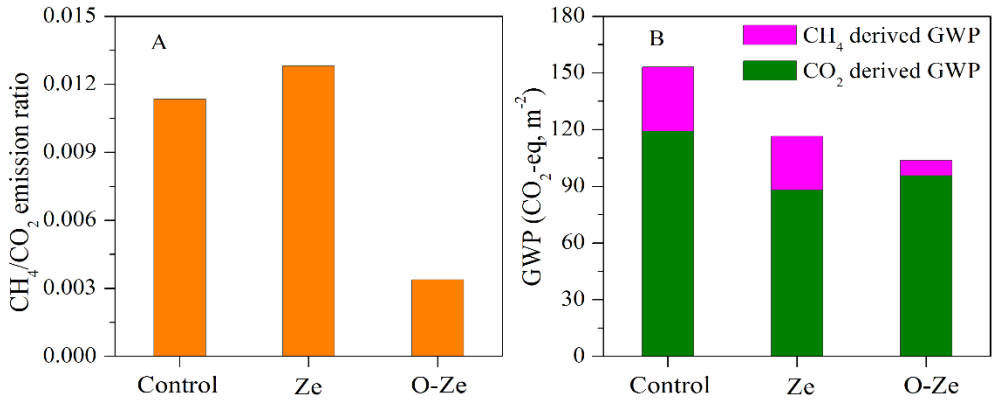

Figure 3. CH_4/CO_2 emission ratios and total GWP values over the 20-d incubation period. (A) CH_4/CO_2 emission ratio. (B) GWP values. CH_4 is converted to CO_2 equivalent based on the effect of CH_4 on radiative forcing of the atmosphere relative to the effect of CO_2. The GWP of CH_4 is approximately 25 times higher than CO_2 on a mass basis over a hundred-year horizon. CH_4 emissions were multiplied by a factor of 25, and combined with measured CO_2 emissions to estimate the total GWP of each treatment.

Microbial Process Manipulation. To elucidate the mechanism of this observation, we quantified methanogens and methanotrophs using the qPCR method based on the methanogenic archaeal 16S rRNA gene and methanotrophic *pmoA* gene, respectively.[22-24] In the control system, methanogen abundance increased following the algal deposition. The archaeal 16S rRNA gene increased from 0.12×10^6 to 0.20×10^6 copies L^{-1} in the water column (Figure 4A), and from 4.12×10^6 to 5.71×10^6 copies g^{-1} in the surface sediment (Figure 4C) on day 7, which potentially contributed to the high CH_4 emissions (Figure 2). After algal deposition, the zeolite addition in the Ze system increased methanotroph

231 abundance (Figure 4D,F); however, methanogen blooms occurred in both the zeolite layer
232 and surface sediment, which could be potentially responsible for massive CH_4 production.
233 The archaeal 16S rRNA gene reached 0.17×10^6 and 5.55×10^6 copies g^{-1} on day 20 in the
234 zeolite layer (Figure 4B) and surface sediment (Figure 4C) in the Ze treatment, respectively.
235 When oxygen nanobubbles enriched zeolites were used in the O-Ze treatment, methanogen
236 abundance declined in both the zeolite layer and surface sediment compared with when
237 zeolites without oxygen nanobubbles were used in the Ze treatment. The archaeal 16S
238 rRNA gene in the O-Ze treatment reached 0.01×10^6 and 4.35×10^6 copies g^{-1} on day 20
239 in the zeolite layer and surface sediment, respectively (Figure 4B,C). Moreover, the
240 methanotroph abundance in the O-Ze treatment was further increased in the zeolite layer
241 compared with when zeolites without oxygen nanobubbles were used in the Ze treatment.
242 The *pmoA* gene reached 0.12×10^6 copies g^{-1} on day 7, and 0.10×10^6 copies g^{-1} on day
243 20 in the O-Ze treatment, while it was only 0.01×10^6 copies g^{-1} on day 7 and 0.07×10^6
244 copies g^{-1} on day 20 in the Ze treatment (Figure 4E,F). In natural waters, CH_4 is mainly
245 produced by anaerobic methanogens, and then partially oxidized to CO_2 by aerobic
246 methanotrophs before it is emitted into the atmosphere.[30-32] Surface oxygen nanobubbles
247 potentially served as oxygen suppliers to the surroundings. The created oxygen enriched
248 environment (Figure 1) favored methanotroph growth and simultaneously inhibited
249 methanogen growth (Figure 4),[33] leading to relatively lower CH_4 emissions and higher CO_2
250 emissions than the zeolites without oxygen nanobubbles (Figure 2).

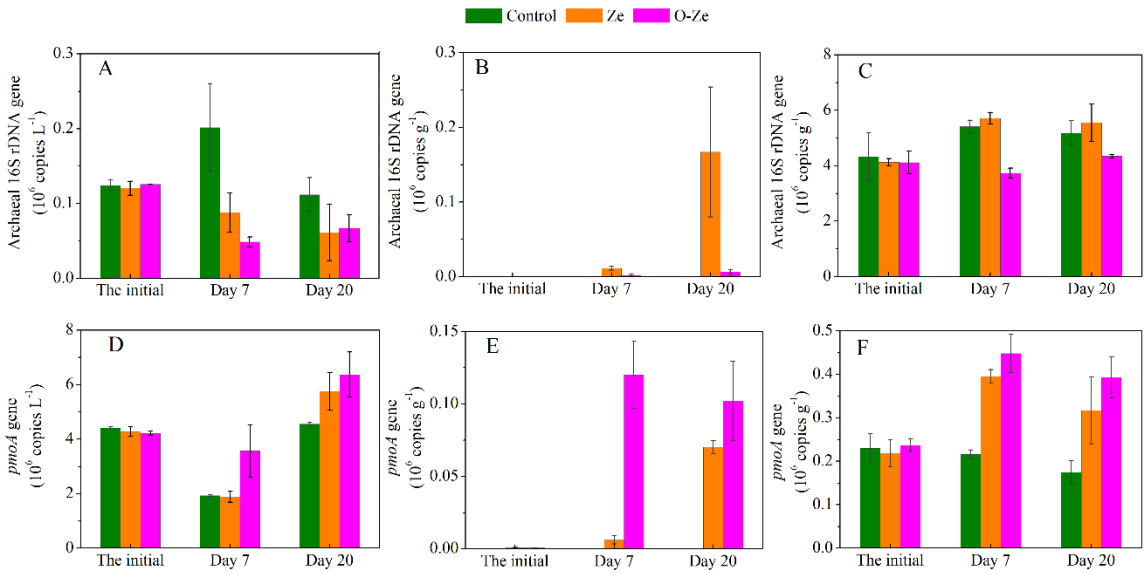

Figure 4. Abundances of methanogens and methanotrophs in the column simulation systems. Methanogens and methanotrophs were quantified using the q-PCR method based on the archaeal 16S rRNA and *pmoA* genes, respectively. The surface sediment in the Ze and O-Ze referred to the sediment below the zeolite layer. (A) archaeal 16S rRNA gene in the water column; (B) archaeal 16S rRNA gene in the zeolite layer; (C) archaeal 16S rRNA gene in the surface sediment; (D) *pmoA* gene in the water column; (E) *pmoA* gene in the zeolite layer; (F) *pmoA* gene in the surface sediment. Error bars indicate standard deviations.

Implications for Geo-engineering in Hypoxic/anoxic Waters. When eutrophication occurs, algae often proliferate as dense floating mats.[34,35] When these blooms die, they sink to the bottom sediment and decay, causing hypoxia/anoxia[8,36,37] and thereby stimulating CH_4 production.[38,39] Our results suggest a possible principle for hypoxia/anoxia remediation in natural waters. However, existing technological principles in oxygen delivery are limited to aeration and mixing,[4,5,40] which fundamentally prevent their large-

scale application in hypoxic/anoxic waters that are crucial to the environment. Suspended solids can be flushed through rivers to lakes and coastal waters and gradually settle onto the bottom sediment.[41,42] If oxygen enriched clay particles can be continuously dispensed through the inflowing rivers, it may provide a geo-engineering method for oxygen delivery especially to the deep waters and sediments. In recent years, geo-engineering methods have proved to be feasible in fixing natural water problems.[18,43,44] But it still remains a challenge to deliver safe materials (such as clays) cost-effectively into natural water systems. Compared with artificial aeration and mixing, surface oxygen nanobubble delivery should not alter stratification or circulation patterns in the water, but instead follow a natural settling process. Previous studies have indicated that oxygen nanobubbles can remain stable in water for a prolonged period (weeks or months) compared with microbubbles.[11,45] If they can be dispensed slowly but continuously, they may serve as potential oxygen suppliers for remediating anoxic sediment, which would cause a series of changes in the nitrogen, phosphorus and sulfur cycles in receiving waters.[46-48] However, there may be some problems to solve before the large-scale field applications of this method, such as ecological impacts and the dosage of zeolites. It is possible to increase the amount of oxygen absorbed by increasing the porosity of zeolites or screen other effective materials as oxygen carriers (e.g., ecologically safe sediments), however, this requires further studies.

ACKNOWLEDGMENTS

This study is supported by the National Key R&D Program of China (2017YFA0207204, 201707-2021.6) and National Natural Science Foundation of China (91547206, 51709181, 41701112). We thank Samantha Best for proofreading the English

Supporting Information

The system for the analysis of oxygen absorption capacity of zeolites, the algal water-sediment simulation cylinders used in this study.

REFERENCES

(1) Schwarz, J. I. K.; Eckert, W.; Conrad, R. Response of the methanogenic microbial community of a profundal lake sediment (Lake Kinneret, Israel) to algal deposition. *Limnol. Oceanogr.* **2008**, 53, (1), 113-121.

(2) West, W. E.; Coloso, J. J.; Jones, S. E. Effects of algal and terrestrial carbon on methane production rates and methanogen community structure in a temperate lake sediment. *Freshwater Biol.* **2012**, 57, (5), 949-955.

(3) Wang, H. J.; Dai, M. H.; Liu, J. W.; Kao, S. J.; Zhang, C.; Cai, W. J.; Wang J. Z.; Qian, W.; Zhao, M. X.; Sun, Z. Eutrophication-driven hypoxia in the East China Sea off the Changjiang Estuary. *Environ. Sci. Technol.* **2016**, 50, (5), 2255-2263.

(4) Beutel, M. W. Inhibition of ammonia release from anoxic profundal sediments in lakes using hypolimnetic oxygenation. *Ecol. Eng.* **2006**, 28, (3), 271-279.

307 (5) Gantzer, P. A.; Bryant, L. D.; Little, J. C. Effect of hypolimnetic oxygenation on oxygen
308 depletion rates in two water-supply reservoirs. *Water Res.* **2009**, 43, (6), 1700-1710.
309 (6) Gerling, A. B.; Browne, R. G.; Gantzer, P. A.; Mobley, M. H.; Little, J. C.; Carey, C. C.
310 First report of the successful operation of a side stream supersaturation hypolimnetic
311 oxygenation system in a eutrophic, shallow reservoir. *Water Res.* **2014**, 67, 129-143.
312 (7) Munger, Z. W.; Carey, C. C.; Gerling, A. B.; Hamre, K. D.; Doubek, J. P.; Klepatzki, S.
313 D.; McClure, R. P.; Schreiber, M. E. Effectiveness of hypolimnetic oxygenation for
314 preventing accumulation of Fe and Mn in a drinking water reservoir. *Water Res.* **2016**, 106,
315 1-14.
316 (8) Conley, D. J. Save the Baltic Sea. *Nature* **2012**, 486, (7404), 463-464.
317 (9) Stigebrandt, A.; Gustafsson, B. G. Improvement of Baltic proper water quality using
318 large-scale ecological engineering. *Ambio* **2007**, 36, (2-3), 280-286.
319 (10) Agarwal, A.; Ng, W. J.; Liu, Y. Principle and applications of microbubble and
320 nanobubble technology for water treatment. *Chemosphere* **2011**, 201684, (9), 1175-1180.
321 (11) Ebina, K.; Shi, K.; Hirao, M.; Hashimoto, J.; Kawato, Y.; Kaneshiro, S.; Morimoto, T.;
322 Koizumi, K.; Yoshikawa, H. Oxygen and air nanobubble water solution promote the growth
323 of plants, fishes, and mice. *PlOS ONE* **2013**, 8, (6).
324 (12) Seddon, J. R. T.; Lohse, D.; Ducker, W. A.; Craig, V. S. J.; A deliberation on
325 nanobubbles at surfaces and in bulk. *Chemphyschem.* **2012**, 13, (8), 2179-2187.
326 (13) Meng, P.; Deng, S.; Lu, X.; Du, Z.; Wang, B.; Huang, J.; Wang, Y.; Yu, G.; Xing, B.
327 Role of air bubbles overlooked in the adsorption of perfluorooctanesulfonate on

328 hydrophobic carbonaceous adsorbents. *Environ. Sci. Technol.* **2014**, 48, (23), 13785-13792.
329 (14) Wang, L.; Miao, X.; Pan, G. Microwave-induced interfacial nanobubbles. *Langmuir*
330 **2016**, 32, (43), 11147-11154.
331 (15) Pan, G.; He, G.; Zhang, M.; Zhou, Q.; Tyliszczak, T.; Tai, R.; Guo, J.; Bi, L.; Wang,
332 L.; Zhang, H. Nanobubbles at hydrophilic particle - water interfaces. *Langmuir* **2016**, 32,
333 (43), 11133-11137.
334 (16) Pan, G.; Yang, B. Effect of surface hydrophobicity on the formation and stability of
335 oxygen nanobubbles. *Chemphyschem.* **2012**, 13, (8), 2205-2212.
336 (17) Shi, W.; Tan, W.; Wang, L.; Pan, G. Removal of *Microcystis aeruginosa* using cationic
337 starch modified soils. *Water Res.* **2016**, 97, 19-25.
338 (18) Pan, G.; Yang, B.; Wang, D.; Chen, H.; Tian, B.; Zhang, M.; Yuan, X.; Chen, J. In-
339 lake algal bloom removal and submerged vegetation restoration using modified local soils.
340 *Ecol. Eng.* **2011**. 37, (2), 302-308.
341 (19) Duchemin, E.; Lucotte, M.; Canuel, R. Comparison of static chamber and thin
342 boundary layer equation methods for measuring greenhouse gas emissions from large water
343 bodies. *Environ. Sci. Technol.* **1999**, 33, (2), 350-357.
344 (20) Stocker, T. Climate change 2013: the physical science basis: *Working Group I*
345 *contribution to the Fifth assessment report of the Intergovernmental Panel on Climate*
346 *Change*. Cambridge University Press: Cambridge, U.K., **2014**.
347 (21) Holgerson, M. A.; Raymond, P. A. Large contribution to inland water CO_2 and CH_4
348 emissions from very small ponds. *Nat. Geosci.* **2016**, 9, (3), 222-226.

(22) Watanabe, T.; Kimura, M.; Asakawa, S. Dynamics of methanogenic archaeal communities based on rRNA analysis and their relation to methanogenic activity in Japanese paddy field soils. *Soil Biol. Biochem.* **2007**, 39, (11), 2877-2887.

(23) Ma, K.; Lu, Y. Regulation of microbial methane production and oxidation by intermittent drainage in rice field soil. *FEMS Microbiol. Ecol.* **2011**, 75, (3), 446-456.

(24) Shi, W.; Chen, Q.; Yi, Q.; Yu, J.; Ji, Y.; Hu, L.; Chen, Y. Carbon emission from cascade reservoirs: Spatial heterogeneity and mechanisms. *Environ. Sci. Technol.* **2017**, 51, (21), 12175-12181.

(25) Bocaniov, S. A.; Scavia, D. Temporal and spatial dynamics of large lake hypoxia: Integrating statistical and three-dimensional dynamic models to enhance lake management criteria. *Water Resour. Res.* **2016**, 52, (6), 4247-4263.

(26) Mallin, M. A.; Johnson, V. L.; Ensign, S. H.; MacPherson, T. A. Factors contributing to hypoxia in rivers, lakes, and streams. *Limnol. Oceanogr.* **2006**, 51, (1), 690-701.

(27) Scavia, D.; Donnelly, K. A. Reassessing hypoxia forecasts for the Gulf of Mexico. *Environ. Sci. Technol.* **2007**, 41, (23), 8111-8117.

(28) Paerl, H. W.; Paul, V. J. Climate change: links to global expansion of harmful cyanobacteria. *Water Res*. **2012**, 46, (5), 1349-1363.

(29) Pan, G.; Dai, L. C.; Li, L.; He, L. C.; Li, H.; Bi, L.; Gulati, R. D. Reducing the recruitment of sedimented algae and nutrient release into the overlying water using modified soil/sand flocculation-capping in eutrophic lakes. *Environ. Sci. Technol.* 2012, 46, (9), 5077-5084.

(30) Borrel, G.; Jezequel, D.; Biderre-Petit, C.; Morel-Desrosiers, N.; Morel, J. P.; Peyret, P.; Fonty, G.; Lehours, A. C. Production and consumption of methane in freshwater lake ecosystems. *Res. Microbiol.* **2011**, 162, (9), 832-847.

(31) Deutzmann, J. S.; Stief, P.; Brandes, J.; Schink, B. Anaerobic methane oxidation coupled to denitrification is the dominant methane sink in a deep lake. *P. Natl. Acad. Sci. USA* **2014**, 111 (51), 18273-18278.

(32) Felden, J.; Wenzhöfer, F.; Feseker, T.; Boetius, A. Transport and consumption of oxygen and methane in different habitats of the Håkon Mosby Mud Volcano (HMMV). *Limnol. Oceanogr.* **2010**, 55, (6), 2366-2380.

(33) Billard, E.; Domaizon, I.; Tissot, N.; Arnaud, F.; Lyautey, E. Multi-scale phylogenetic heterogeneity of archaea, bacteria, methanogens and methanotrophs in lake sediments. *Hydrobiologia* **2015**, 751, (1), 159-173.

(34) Paerl, H.W.; Huisman, J. Climate - Blooms like it hot. *Science* **2008**, 320, (5872), 57-58.

(35) Duan, H.; Ma, R.; Xu, X.; Kong, F.; Zhang, S.; Kong, W., Hao, J.; Shang, L. Two-decade reconstruction of algal blooms in China's Lake Taihu. *Environ. Sci. Technol.* **2009**, 43, (10), 3522-3528.

(36) Rosenberg, R.; Elmgren, R.; Fleischer, S.; Jonsson, P.; Persson, G.; Dahlin, H. Marine eutrophication case - Studies in Sweden. *Ambio* **1990**, 19, (3), 102-108.

(37) Watson, S. B.; Miller, C.; Arhonditsis, G.; Boyer, G. L.; Carmichael, W.; Charlton, M. N.; Confesor, R.; Depew, D. C.; Höök, T. O.; Ludsin, S. A.; Matisoff, G.; McElmurry, S.

391 P.; Murray, M. W.; Richards, R. P.; Rao, Y. R.; Steffen, M. M.; Wilhelm, S. W. The re-
392 eutrophication of Lake Erie: harmful algal blooms and hypoxia. *Harmful Algae* **2016**, 56,
393 44-66.
394 (38) Naqvi, S. W. A.; Bange, H. W.; Farias, L.; Monteiro, P. M. S.; Scranton, M. I.; Zhang,
395 J. Marine hypoxia/anoxia as a source of CH_4 and N_2O. *Biogeosciences* 2010, 7, (7), 2159-
396 2190.
397 (39) Gulzow, W.; Grawe, U.; Kedzior, S.; Schmale, O.; Rehder, G. Seasonal variation of
398 methane in the water column of Arkona and Bornholm Basin, western Baltic Sea. *J. Marine*
399 *Syst.* **2014**. 139, 332-347.
400 (40) Cowell, B. C.; Dawes, C. J.; Gardiner, W. E.; Scheda, S. M. The influence of whole
401 lake aeration on the limnology of a hypereutrophic lake in central florida. *Hydrobiologia*
402 **1987**, 148, (1), 3-24.
403 (41) Pan, G.; Krom, M. D.; Zhang, M.; Zhang, X.; Wang, L.; Dai, L.; Sheng, Y.; Mortimer,
404 R. J. G. Impact of suspended inorganic particles on phosphorus cycling in the Yellow River
405 (China). *Environ. Sci. Technol.* **2013**, 47, (17), 9685-9692.
406 (42) Yi, Q.; Chen, Q.; Shi, W.; Lin, Y.; Hu, L. Sieved transport and redistribution of
407 bioavailable phosphorus from watershed with complex river networks to lake. *Environ. Sci.*
408 *Technol.* **2017**, 51, (18), 10379-10386.
409 (43) Mackay, E. B.; Maberly, S. C.; Pan, G.; Reitzel, K.; Bruere, A.; Corker, N.; Douglas,
410 G.; Egemose, S.; Hamilton, D.; Hatton-Ellis, T.; Huser, B.; Li, W.; Meis, S.; Moss, B.;
411 Lurling, M.; Phillips, G.; Yasseri, S.; Spears, B. M. Geoengineering in lakes: welcome

412 attraction or fatal distraction? *Inland Waters* **2014**, 4, (4), 349-356.

413 (44) Spears, B. M.; Dudley, B.; Reitzel, K.; Rydin, E. Geo-engineering in lakes - A call for

414 consensus. *Environ. Sci. Technol.* 2013, 47, (9), 3953-3954.

415 (45) Ohgaki, K.; Khanh, N. Q.; Joden, Y.; Tsuji, A.; Nakagawa, T. Physicochemical

416 approach to nanobubble solutions. *Chem. Eng. Sci.* **2010**, 65, (3), 1296-1300.

417 (46) Kessler, A. J.; Glud, R. N.; Cardenas, M. B.; Cook, P. L. Transport zonation limits

418 coupled nitrification-denitrification in permeable sediments. *Environ. Sci. Technol.* **2013**,

419 47, (23), 13404-13411.

420 (47) Schroth, A. W.; Giles, C. D.; Isles, P. D.; Xu, Y.; Perzan, Z.; Druschel, G. K. Dynamic

421 coupling of iron, manganese, and phosphorus behavior in water and sediment of shallow

422 ice-covered eutrophic lakes. *Environ. Sci. Technol.* **2015**, 49, (16), 9758-9767.

423 (48) Fisher, J. C.; Wallschläger, D.; Planer-Friedrich, B.; Hollibaugh, J. T. A new role for

424 sulfur in arsenic cycling. *Environ. Sci. Technol.* **2007**, 42, (1), 81-85.